A&A 506, 95–101 (2009)
DOI: 10.1051/0004-6361/200911928

The CoRoT space mission: early results

Astronomy & Astrophysics
Special feature

The B0.5IVe CoRoT target HD 49330⋆

I. Photometric analysis from CoRoT data

A.-L. Huat[1], A.-M. Hubert[1], F. Baudin[2], M. Floquet[1], C. Neiner[1], Y. Frémat[3,1], J. Gutiérrez-Soto[1], L. Andrade[4], B. de Batz[1], P. D. Diago[5], M. Emilio[6], F. Espinosa Lara[1], J. Fabregat[5], E. Janot-Pacheco[4], B. Leroy[7], C. Martayan[3,1], T. Semaan[1], J. Suso[5], M. Auvergne[7], C. Catala[7], E. Michel[7], and R. Samadi[7]

[1] GEPI, Observatoire de Paris, CNRS, Université Paris Diderot, 5 place Jules Janssen, 92190 Meudon, France
e-mail: anne-laure.huat@obspm.fr
[2] Institut d'Astrophysique Spatiale (IAS), Bâtiment 121, 91405 Orsay Cedex, France
[3] Royal Observatory of Belgium, 3 avenue circulaire, 1180 Brussel, Belgium
[4] University of Sao Paulo, Brasil
[5] Observatori Astronòmic de la Universitat de València, ED. Instituts d'Investigació, Poligon La Coma, 46980 Paterna, València, Spain
[6] Obervatório Asrtonômico, Universidade Estadual de Ponta Grossa, Av. Carlos Cavalcanti, 4748 Ponta Grossa, Paraná, Brazil
[7] LESIA, Observatoire de Paris, CNRS, UPMC, Université Paris Diderot, 5 place Jules Janssen, 92190 Meudon, France

Received 23 February 2009 / Accepted 5 June 2009

ABSTRACT

Context. Be stars undergo outbursts producing a circumstellar disk from the ejected material. The beating of non-radial pulsations has been put forward as a possible mechanism of ejection.
Aims. We analyze the pulsational behavior of the early B0.5IVe star HD 49330 observed during the first CoRoT long run towards the Galactical anticenter (LRA1). This Be star is located close to the lower edge of the β Cephei instability strip in the HR diagram and showed a 0.03 mag outburst during the CoRoT observations. It is thus an ideal case for testing the aforementioned hypothesis.
Methods. We analyze the CoRoT light curve of HD 49330 using Fourier methods and non-linear least square fitting.
Results. In this star, we find pulsation modes typical of β Cep stars (p modes) and SPB stars (g modes) with amplitude variations along the run directly correlated with the outburst. These results provide new clues about the origin of the Be phenomenon as well as strong constraints on the seismic modelling of Be stars.

Key words. stars: early-type – stars: emission-line, Be – stars: individual: HD 49330 – stars: rotation – stars: oscillations

1. Introduction

Among massive stars, Be stars are of particular interest for studying the pulsational properties of rapid rotators. Be stars are main-sequence or slightly evolved B stars surrounded by an equatorially concentrated envelope, which is fed by discrete mass-loss events. Although Be stars are rapid rotators, their rotational velocity does not reach the break-up velocity and the causes of non-regular mass loss in these stars are still unknown. In these stars rotating at about 90% of the critical velocity (Frémat et al. 2005), non-radial pulsations could be efficient for providing the additional amount of angular momentum needed to eject material. CoRoT provides an opportunity to assess the role of non-radial pulsations in the activity of Be stars.

This paper is dedicated to HD 49330 (V739 Mon), the first early Be star observed by CoRoT in the LRA1 seismology field. We first present the previous seismic results obtained for HD 49330 from space and ground-based observations (Sect. 2). In Sect. 3, we describe the CoRoT observations of this star. We then summarize in Sect. 4 the different methods used to analyse the CoRoT light curve of HD 49330 and present our results in Sect. 5. We discuss the results obtained for this star and their interpretation in term of pulsations in Sect. 6. Finally, conclusions are presented in Sect. 7.

2. HD 49330: parameters and known variability

HD 49330 is a rapidly rotating very early Be star (B0.5IVe). Its fundamental parameters have been determined by Frémat et al. (2006) and confirmed using high-resolution spectra (Floquet et al. 2009, hereafter Paper II). The effective temperature is $T_{\rm eff}$ = 27 000 ± 500 K and log g = 3.8 ± 0.2 for an angular velocity between 0.9 and 0.99 of the critical angular velocity. The measured $v \sin i$ is 270 km s^{-1} (see Table 2 in Floquet et al. 2009, hereafter Paper II).

Like almost all early Be stars (Hubert & Floquet 1998), HD 49330 is very active. The star is known to exhibit light variability on several timescales and to undergo outbursts. Gutiérrez-Soto et al. (2007) investigated the variability of HD 49330 using data acquired by a 4-year campaign at the Observatorio de Sierra Nevada (OSN) and large datasets provided by the Hipparcos mission and the All Sky Automated Survey (ASAS-3) (Pojmanski 2002).

⋆ Tables 3 to 7 are only available in electronic form at the CDS via anonymous ftp to cdsarc.u-strasbg.fr (130.79.128.5) or via
http://cdsweb.u-strasbg.fr/cgi-bin/qcat?J/A+A/506/95

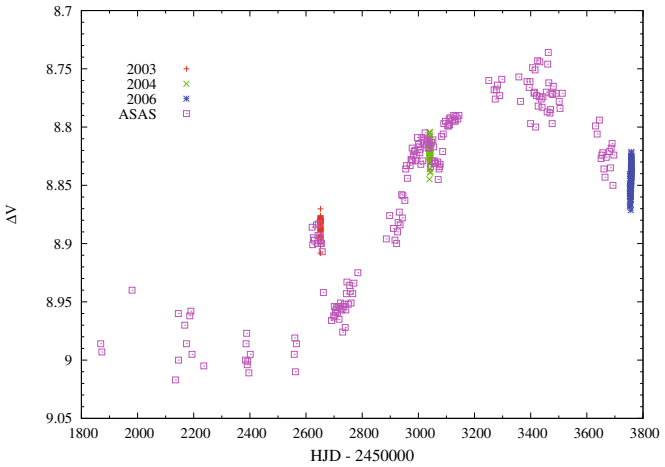

Fig. 1. Variability in the *V* magnitude of HD 49330 from ASAS-3 and OSN data obtained in 2003, 2004, and 2006.

The light curve of ASAS-3 (Fig. 1) shows a quasi-cyclical variation of about 1600 days, and includes events of shorter duration. In particular, an outburst of about 200 days occurred around JD = 2 452 640. A fading may have also been observed at about JD = 2 453 050. The observations of both outbursts and fadings in the same star are puzzling since fadings are usually considered as outbursts observed from a particular angle. This suggests that the material producing the observed outburst and fading in HD 49330 has not been ejected by the star at the same latitude.

The Hipparcos data obtained between 1989 and 1993 show a rapid variability with a frequency 3.53 c.d^{-1}. The data of the three seasons 2003, 2004, and 2006 (see Fig. 1) acquired at OSN (Observatorio de Sierra Nevada) allowed Gutiérrez-Soto et al. (2007) to detect a frequency at 2.13 c.d^{-1}. According to the authors, this frequency has been found in the data collected during three years in the V filter, but its amplitude has changed dramatically, from 13 mmag in 2003 to 4 mmag in 2004 and 8 mmag in 2006.

3. Observations

3.1. CoRoT photometric observations

HD 49330 was observed during the first long run of the CoRoT mission in the anticenter direction (LRA1) from October 18, 2007 to March 3, 2008 (i.e. for 136.886 days) with a time sampling of 1 s. We note that the data delivered were resampled by a mean over 32 s. This stellar field is centered on α = 06$^{\rm h}$ 47$^{\rm m}$ 57.27$^{\rm s}$, δ = 00° 46′34.02″. The time origin of the observations, JD$_{\rm init}$ = 2 454 391.95. An interruption in the observations caused by a failure of one of the data process units occurred during the run. This loss of data was detected around JD–JD$_{\rm init}$ = 92 and lasted 3.53 days.

The photometric data presented in this paper were reduced with the CoRoT pipeline (Samadi et al. 2006; Appourchaux et al. 2008). This pipeline provides a correction for the CCD zero offset and gain, the orbital and the background perturbations, and the variation in the integrating time. It also suppress outliers. A correction for the loss of gain due to CCD and/or optics ageing was then applied. The resulting light curve is shown in Fig. 2.

In this light curve, we see an increase in brightness (also called light outburst) of 0.03 mag. The behavior of the light outburst of HD 49330 is similar to those observed in other early Be

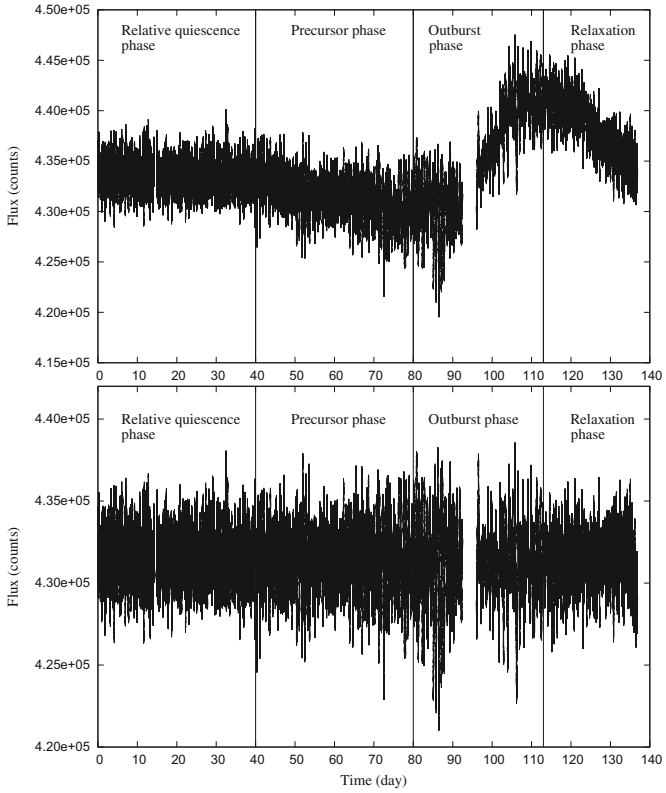

Fig. 2. *Top panel*: CoRoT light curve of HD 49330 in flux. The light curve was corrected for the loss in CCD gain. *Bottom panel*: light curve of HD 49330 detrended from the shape of the outburst. The time origin is JD = 2 454 391.95

stars, e.g., 66 Oph (Floquet et al. 2002) and υ Cyg (Neiner et al. 2005).

Outbursts are episodes of enhanced mass transfer from the star to the disk, commonly observed in hot Be stars. The description of an outburst has only been provided spectroscopically by the study of line emission. A schematic picture of the different phases of a line emission outburst was established for the Be star μ Cen by Rivinius et al. (1998). By analogy with the spectroscopic description of an outburst, we identified four parts of the light outburst depicted by the CoRoT data: (1) a phase of relative quiescence at JD–JD$_{\rm init}$ = [0–40]; (2) a decrease in the flux that we call the precursor phase at JD–JD$_{\rm init}$ = [40–80]; (3) the outburst characterized by the sudden increase in flux at JD–JD$_{\rm init}$ = [80–113]; and finally (4) a relaxation phase where the star slowly comes back to the phase of relative quiescence at JD–JD$_{\rm init}$ = [113–139].

3.2. Simultaneous spectroscopic observations

Ground-based high-resolution spectroscopic observations (FEROS mounted of the telescope La Silla, Chile and Narval mounted of the telescope TBL, Pic du Midi, France) were carried simultaneously with the CoRoT observations at two epochs: JD–JD$_{\rm init}$ = [56–72] and [85–88], (see Paper II). These spectroscopic observations were obtained during the precursor phase of the outburst, i.e., just before the increase in flux due to the outburst itself. These data are analyzed in detail in Paper II.

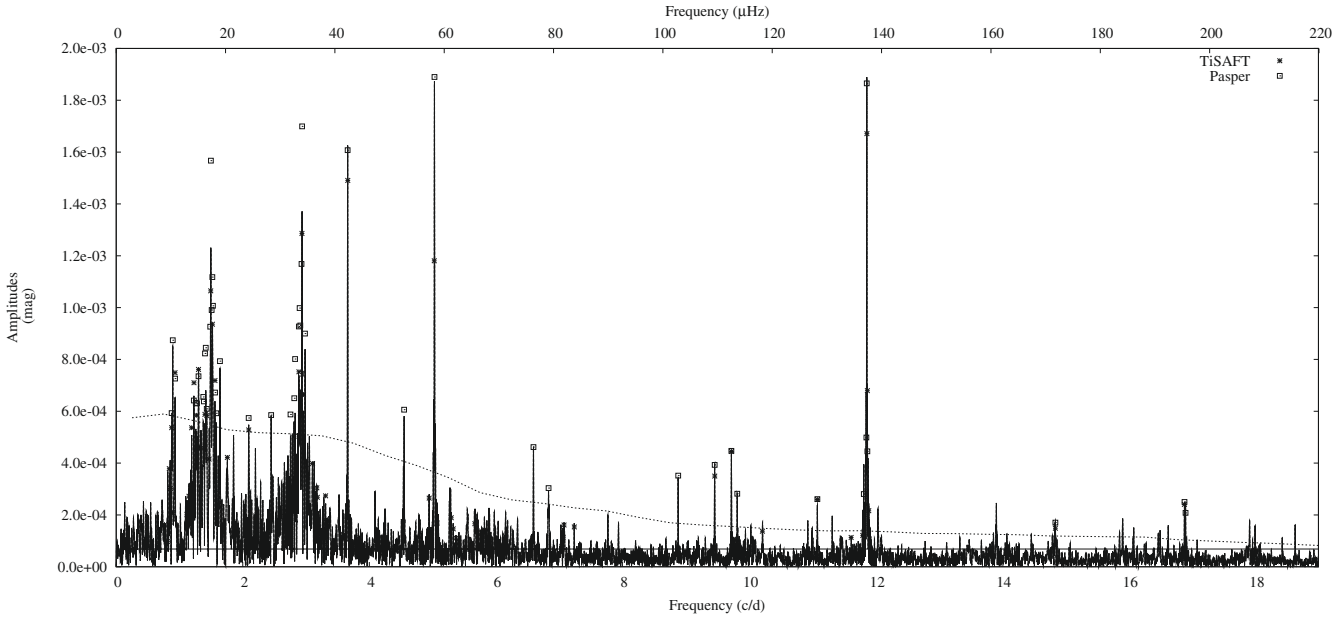

Fig. 3. Power spectrum of HD 49330 derived from the CoRoT light curve. Frequencies found by the TiSAFT and Pasper codes have been reported on the spectra. The dashed line corresponds to the limit of significance for Pasper i.e. $S/N > 4$ and the solid line is the limit of significance for TiSAFT with $P = 99\%$

4. Analysis methods

To analyze the CoRoT light curve of HD 49330, we use three codes developed by the CoRoT Be team to search for the frequencies of variations in photometric time series: Pasper, TiSAFT, and Clean-NG. These codes are all based on Fourier analysis but have some differences, in particular, in the stopping criterion used for the frequency search. All amplitudes and phases given in this paper were computed using the Amphi code. The time origin for the phases was assumed to be equal to JD_{init} for each use of Amphi. For a complete description of these methods, we refer to Gutiérrez-Soto et al. (2009). We also use two time-frequency analysis codes to analyze the evolution in the frequency amplitudes.

The first method adopted is based on a wavelet analysis, using the well known Morlet wavelet. It was described and applied to solar seismic data in Baudin et al. (1994) and Baudin et al. (1996). The use of the Morlet wavelet allows the most effective trade-off in terms of frequency resolution and time resolution. The frequency resolution (the full width at half maximum of the wavelet in the Fourier domain) used in the present case is 2 μHz, corresponding to a time resolution of ~5 days.

The second method uses a sliding square box window of a chosen time length and performs the Fourier analysis using one of the three codes (Pasper, TiSAFT, or Clean-NG) in each window. The window size used in this analysis is 4 days, the sliding step is equal to 1 day, we used Clean-NG and recalculated the amplitudes with Amphi.

5. Seismic analysis of CoRoT light curve

We performed several analyses of the light curve: firstly, an analysis of the entire light curve; secondly, an analysis of each of the four parts of the light curve as defined in Sect. 2; and finally, a time-frequency analysis.

5.1. Analysis of the complete light curve

The presence of an outburst during two thirds of the CoRoT run introduces slow and non-sinusoidal variations into the light curve and therefore low frequencies in the Fourier spectrum. We first removed the general trend in the light curve to clean the Fourier spectrum of low frequencies because of this effect (see the bottom panel of Fig. 2). The detrending enhances all small amplitude components of the light curve. We note, in particular, the increase in the oscillation amplitudes just before the rising of the outburst.

We performed a seismic analysis of the detrended light curve of HD 49330 with the three codes described in Sect. 4. The resulting Fourier spectrum is shown in Fig. 3. The amplitudes corresponding to the detected frequencies are given in units of magnitude. The resolution in the frequency determination is $1/2T = 0.0037$ c.d^{-1}, where T is the total duration of the light curve in days (Kallinger et al. 2008).

Many frequencies with a high signal-to-noise ratio are detected in the light curve of HD 49330. These frequencies are distributed among three groups around 0.87 c.d^{-1}, 1.47 c.d^{-1}, and 2.94 c.d^{-1}, and several other isolated frequencies such as 11.86 c.d^{-1}, the main frequency in the Fourier spectrum, 5.03 c.d^{-1}, 3.65 c.d^{-1}, 1.29 c.d^{-1}, and 16.89 c.d^{-1}. We note that the 5.03 c.d^{-1} frequency equals the difference between the 11.86 and 16.89 c.d^{-1} frequencies. The validity of the 5.03 c.d^{-1} or 16.89 c.d^{-1} is discussed in Sect. 6.

Peaks corresponding to a combination of other stronger peaks within the frequency resolution of the data (0.0037 c.d^{-1}), and peaks caused by the observing window, and alias peaks were rejected. Only the significant frequencies provided by the Pasper and TiSAFT methods are indicated in Fig. 3. The number of significant frequencies obtained from the three codes varies between 31 (Pasper) and 77 (TiSAFT). Since the Fourier spectrum consists of groups containing many frequencies, the list of the main frequencies obtained with TiSAFT is given in Table 1. All of the significant frequencies cleaned from combination obtained with this method and a confidence level $P = 99\%$ are given online at the CDS (Table 3).

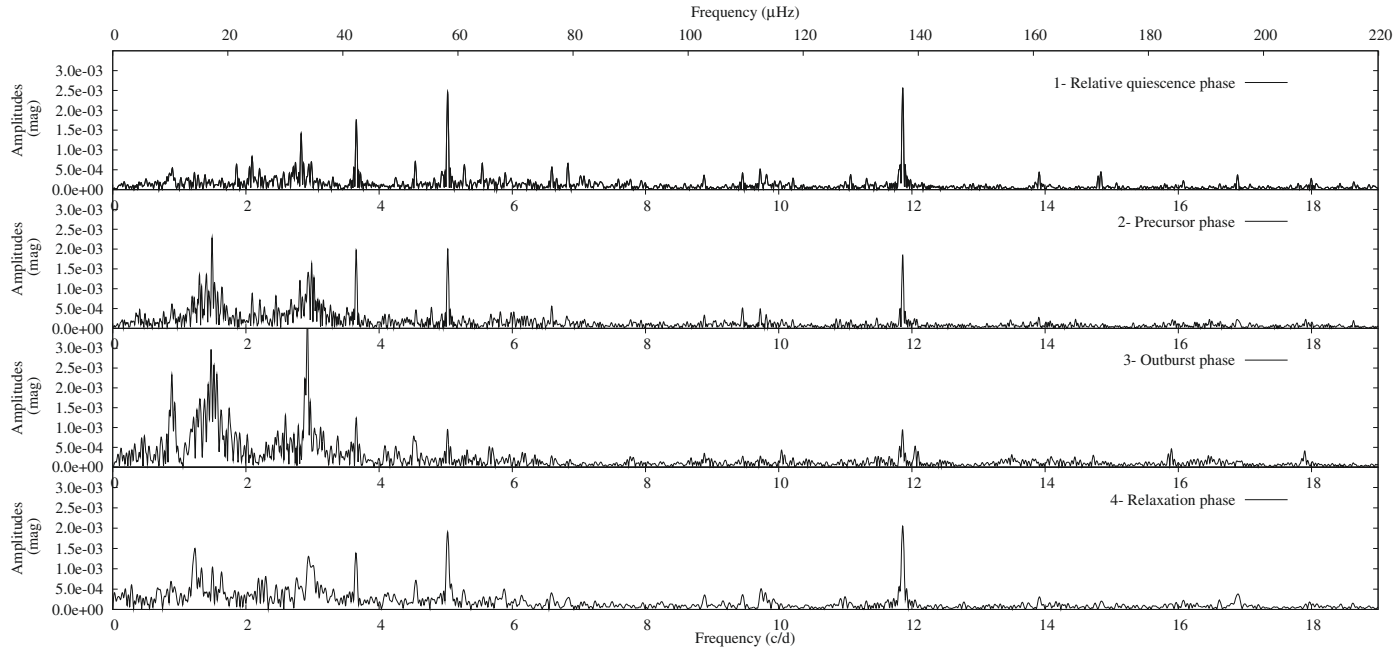

Fig. 4. Power pectrum of the four parts of the light curve of HD 49330. The top panel shows the spectrum of the relative quiescence phase of the light curve at JD–JD$_{init}$ = [0–40], the second panel shows the spectra of the precursor phase at JD–JD$_{init}$ = [40–80], the third panel shows the spectra during the outburst JD–JD$_{init}$ = [80–113], and the bottom panel shows the spectra of the relaxation phase at JD–JD$_{init}$ = [113–139].

Table 1. Main frequencies found by TiSAFT for the global analysis of the light curve of HD 49330.

	Freq. (c.d^{-1})	Amp. mmag	Phase [0, 2π]
F1	11.8639	1.685	3.60
F2	2.9359	1.324	1.88
F3	3.6594	1.509	4.61
F4	5.0260	1.205	3.29
F5	1.4934	1.118	5.82
F6	0.8877	0.186	0.19
F7	1.2289	0.695	5.73
F8	2.8118	0.522	4.07
F9	2.0943	0.566	4.95
F10	1.8552	0.490	3.10
F11	2.6600	0.413	3.75
F12	3.1267	0.312	0.56
F13	2.5636	0.349	2.59
F14	9.4590	0.351	2.30
F15	4.9457	0.281	3.98
F16	3.3092	0.245	1.29
F17	16.8823	0.242	2.56
F18	5.6683	0.170	2.49
F19	6.3410	0.186	1.56
F20	5.2942	0.189	5.28
F21	5.8575	0.168	2.74
F22	7.2395	0.155	6.14
F23	7.0780	0.167	5.69
F24	10.2128	0.149	1.54
Total	TiSAFT: 340, PASPER: 31		

The last line provides the total number of significant frequencies found by each program.

5.2. Analysis of the light curve by parts

For each part of the light curve defined in Sect. 3, i.e., the relative quiescent phase (part 1), precursor phase (part 2), outburst phase (part 3), and relaxation phase (part 4), we performed a new analysis of the detrended light curve using the same methods as in the previous section. The accuracy in the frequency determination is $1/2T$ = 0.013 c.d^{-1}, 0.013 c.d^{-1}, 0.015 c.d^{-1}, and 0.021 c.d^{-1} for each part, respectively.

The resulting Fourier spectra are shown in Fig. 4. We can clearly see a change in the Fourier spectrum from one phase to another. During the precursor and outburst phases, we can indeed see the gradual emergence of the two groups of peaks around 1.47 and 2.94 c.d^{-1}, as well as of some more concentrated frequencies around 0.87 and 1.28 c.d^{-1}, while other frequencies that are dominant during the relative quiescent phase, such as 11.86 c.d^{-1} and 5.03 c.d^{-1}, show a decrease. At the end of the outburst, during the relaxation phase (part 4), the Fourier spectrum seems to recover the former stage depicted in the relative quiescent phase. Some frequencies with weaker amplitudes follow the same behaviour as 11.86 c.d^{-1}, e.g., 9.45 c.d^{-1} and 9.72 c.d^{-1} The number of frequencies detected with PASPER and TISAFT methods for each part of the light curve, and the list of significant independent frequencies obtained with TISAFT are given in Table 2. The entire list of frequencies detected with this method is also given online at the CDS (Tables 4–7).

5.3. Time-frequency analysis

Because a change in amplitude and frequency was observed between the four parts in the previous section (Fig. 4), a time-frequency analysis of the light curve of HD 49330 was performed. This analysis will help us to see the subtleties of variations in amplitude of the frequencies with time. For this purpose, we used the two time-frequency analysis methods described in Sect. 4.

This study confirms that the amplitudes change with time. We can also clearly see a correlation between the change in amplitude and the occurence of the outburst (Fig. 5, top panel). While the main frequencies (11.86 c.d^{-1} and 5.03 c.d^{-1}) show a decrease in amplitude before and during the outburst, many new frequencies emerge in groups around 1.47 c.d^{-1} and 2.94 c.d^{-1}. We note that the 1.47 c.d^{-1} frequency is close to another one at 1.57 c.d^{-1} of similar amplitude, conspicuously present at the

Table 2. The most important frequencies found by TiSAFT for the four parts of the light curve.

	Relative quiescence			Precursor			Outburst			Relaxation		
	Freq. ($c.d^{-1}$)	Amp. mmag	Phase $[0, 2\pi]$	Freq. ($c.d^{-1}$)	Amp. mmag	Phase $[0, 2\pi]$	Freq. ($c.d^{-1}$)	Amp. mmag	Phase $[0, 2\pi]$	Freq. ($c.d^{-1}$)	Amp. mmag	Phase $[0, 2\pi]$
F1	0.5273	0.108	4.49				0.5446	0.555	0.83			
F2	0.8883 (*)	0.546	2.81	0.8750	0.384	1.85	0.8709 (*)	1.606	4.66			
F3				0.9139	0.214	2.87				0.9059	0.419	3.93
F4							0.9461	1.123	0.45			
F5	1.1244	0.382	5.68									
F6	1.1780	0.227	1.46				1.1507	0.796	5.28			
F7							1.2017	0.666	3.90	1.2279 (*)	1.455	0.35
F8	1.2806	0.358	1.49	1.2957 (*)	1.087	1.55	1.2914 (*)	1.226	5.96	1.3171	0.709	5.38
F9				1.5058 (*)	1.289	0.67	1.4986 (*,S)	1.148	3.66	1.4865	0.728	5.98
F10				1.5750	1.020	3.91	1.5739 (*)	1.748	0.79			
F11	1.8640 (*)	0.666	1.99	1.8498	0.508	5.20	1.8461	0.877	2.52	1.8960	0.359	4.01
F12	2.0462	0.571	1.57				2.0390	0.199	0.41			
F13	2.1043 (*)	0.709	3.36	2.1056	0.579	0.72	2.1033	0.042	0.11			
F14				2.2731	0.428	1.88				2.2803	0.438	4.72
F15							2.3138	0.296	2.57			
F16				2.6703	0.731	5.41	2.6679	0.690	4.80			
F17	2.7246 (*)	0.331	1.81	2.734	0.760	3.67	2.7273	0.742	2.61			
F18	2.8333 (*)	1.278	2.64									
F19	2.8682	0.439	0.85	2.8500	0.926	1.02	2.8788 (*)	1.634	2.08			
F20	2.9489	0.621	5.77	2.9423 (*)	1.602	5.37	2.9599	0.502	2.03	2.9570	1.123	5.70
F21							2.9181 (*)	2.924	5.82			
F22	3.0711	0.213	2.52							3.0293	0.691	3.09
F23				3.2734	0.597	6.06	3.2728	0.506	2.71			
F24	3.3088	0.237	1.73							3.3099	0.408	0.43
F25	3.6633 (*)	1.662	4.60	3.6517 (*)	1.812	1.13	3.6686	0.947	5.14	3.6607 (*)	1.278	3.07
F26							4.3002	0.300	1.89			
F27	4.6365	0.201	0.75				4.6381	0.157	4.00			
F28	5.0259 (*)	2.283	2.46	5.0287 (*)	1.951	2.30	5.0337	0.904	5.93	5.0362 (*)	1.771	2.87
F29	5.2759 (*)	0.541	1.50	5.2575	0.343	0.60	5.2426	0.163	4.19			
F30	(*)									5.5434	0.161	0.34
F31										5.7751	0.359	1.83
F32				5.8243	0.388	5.02	5.8472	0.275	3.20			
F33				5.9704	0.264	4.70	5.9629	0.251	2.93			
F34							6.0293	0.180	5.84			
F35	6.3502	0.190	5.70	6.3400	0.338	2.16	6.3214	0.097	1.51			
F36	7.7763	0.218	5.25	7.7735	0.236	5.19						
F37							7.8053	0.211	1.72			
F38				8.8772	0.267	3.18	8.8711	0.170	1.36			
F39	9.4524	0.378	3.32	9.4503	0.443	5.82	9.4543	0.245	4.60	9.4597	0.371	1.05
F40	(*)			9.7254	0.508	5.03	9.7276	0.274	3.05	9.7485	0.454	4.65
F41	9.8131	0.397	0.71	9.8187	0.245	5.68				9.8237	0.193	5.41
F42	10.2191	0.285	0.10	10.1991	0.177	1.14	10.2118	0.186	1.83			
F43	11.8583 (*)	2.386	4.68	11.8471 (*, S)	1.146	3.46	11.8468	0.615	1.27	11.8704 (*)	1.939	4.02
F44				11.8742	1.334	6.27	11.8890 (S)	0.189	0.02			
F45	16.8948	0.357	0.96	16.8838 (S)	0.208	1.63	16.8865	0.234	1.15	16.8919	0.422	0.98
Total	TiSAFT:135, Pasper: 15			TiSAFT:103, Pasper: 9			TiSAFT:76, Pasper: 8			TiSAFT:65, Pasper: 4		

(*) indicates that the frequency was also found by Pasper. (S) means that the frequency was detected in the spectroscopy data by Paper II.

end of the precursor phase and at the beginning of the outburst itself ($JD–JD_{init}$ = [84–104]). Then, the two frequencies 1.47 $c.d^{-1}$ and 1.57 $c.d^{-1}$ gradually vanish as the outburst phase (part 3) develops. In contrast, other frequencies become dominant at that epoch, in particular 1.29 $c.d^{-1}$ and 0.87 $c.d^{-1}$. The latter seems to rapidly decrease at the beginning of the relaxation phase (part 4). After the outburst, we observe that the main frequencies at 11.86 $c.d^{-1}$, 5.03 $c.d^{-1}$, and 16.89 $c.d^{-1}$ recovered their initial amplitude, while the emerging frequency groups around 1.47 $c.d^{-1}$ and 2.94 $c.d^{-1}$, as well as the lower frequencies around 1.29 $c.d^{-1}$ and 0.87 $c.d^{-1}$, decreased in amplitude and finally disappeared (see Figs. 5 and 6).

The structure of the groups of frequencies around 1.47 $c.d^{-1}$ and 2.94 $c.d^{-1}$ is complex with many frequencies. Figure 5 shows the results obtained for these groups with the Morlet wavelet method. The 1.47 $c.d^{-1}$ and 2.94 $c.d^{-1}$ frequencies are almost undetectable during the relative quiescence phase. They then reappear during the precursor phase and begin to oscillate in amplitude and in opposite phase with each other with a period of about 10 days, until an unknown phenomenon perturbs

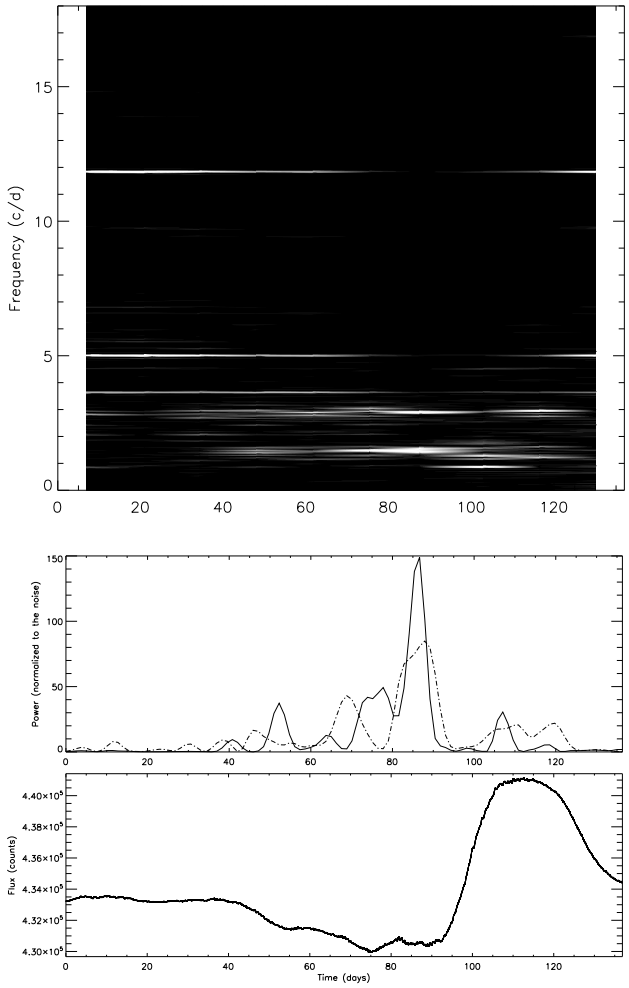

Fig. 5. *Top panel*: evolution in the amplitude Fourier spectrum with time. *Middle panel*: variation in the amplitudes of the 1.47 c.d^{-1} (solid line) and 2.94 c.d^{-1} (dashed line) frequency peaks as a function of time. *Bottom panel*: smoothed light curve of HD 49330. The time origin for all panels correspond to JD = 2 454 391.95.

the 2.94 c.d^{-1} frequency. This perturbation leads to a synchronization of the two frequency variations at a maximum value. Just after the synchronisation, the photometric outburst occurs. We also find that the behaviour of the 1.47 c.d^{-1} frequency is anticorrelated with the total light flux before the epoch of synchronisation: the light flux exhibits secondary minima because the amplitude of the 1.47 c.d^{-1} is at a maximum (see Fig. 5).

6. Discussion

6.1. Pulsation modes

By completing a photometric analysis of the precise CoRoT data acquired over ∼136 days, we were able to detect many different frequencies in the Fourier spectrum. We detected over 300 frequencies in the CoRoT light curve with a 99% probability that these frequencies are not caused to noise. Among them, 30 are independent stellar frequencies including high frequencies and several groups of low frequencies, which are typical of the p and g pulsation modes observed in β Cephei and SPB stars, respectively. It is the first time that such a high number of independent frequencies has been detected in an early Be star.

Some of the frequencies detected with CoRoT have also been detected in photospheric line profile variations with the help of

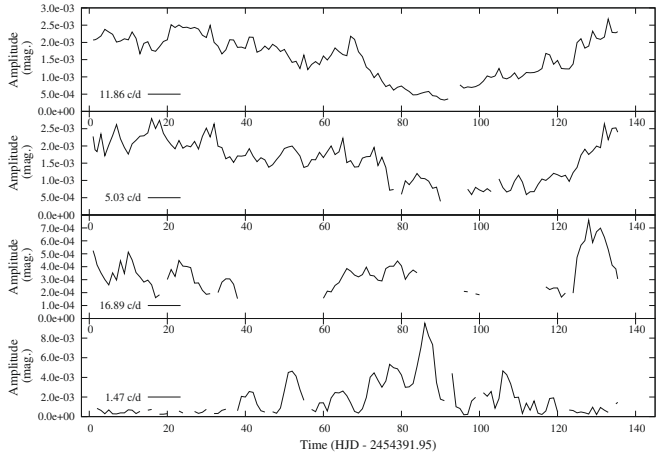

Fig. 6. Variation in the amplitudes as a function of time of four frequencies: 11.86 c.d^{-1}, 5.03 c.d^{-1}, 16.89 c.d^{-1}, and 1.47 c.d^{-1}. We see an anticorrelation between the first two frequencies and the 1.47 c.d^{-1} frequency. The time origin for all panels correspond to JD = 2 454 391.95.

simultaneous spectroscopic observations (Paper II). This spectroscopic study allows us to identify two main frequencies at 11.86 c.d^{-1} and 16.89 c.d^{-1} with intermediate ($\ell \sim 4$) and high degree ($\ell = 6$) p-modes, respectively.

In Paper II, we also proposed to identify the low frequency 1.51 c.d^{-1} with a low degree g-mode. This frequency, as well as the frequency around 2.94 c.d^{-1}, corresponds to a complex group of frequencies. These groups could be the result of pulsation modes with a short lifetime (see below).

The detailed characterization of the pulsation modes of HD 49330, in addition to the fundamental parameters determined by Frémat et al. (2006), provide strong constraints on seismic modelling. In particular, because p and g modes are observed simultaneously in HD 49330, making it a hybrid star, the range of possible seismic models can be narrowed down and we can study the internal structure of this star. Modelling HD 49330 will be the subject of a forthcoming paper.

6.2. Outburst

The light outburst observed in the CoRoT light curve of HD 49330 is typical of the Be phenomenon. Short-lived (days, tens of days), sometimes recurrent, outbursts or/and long-lived outbursts have been detected in Be stars. Even though scenarios have been proposed to model the light curve of long-lived outbursts (Hubert et al. 2000), the physical process responsible for outflows of matter, leading to light outbursts, is poorly understood (Porter & Rivinius 2003).

In addition, the majority of outbursts detected so far in Be stars, using data from the Hipparcos survey and ground-based photometric campaigns, are generally major outbursts with amplitude of several tenths of magnitude. However, major outbursts as in ω CMa in Hipparcos data (Hubert & Floquet 1998) could be preceded by a succession of minor outbursts. The high accuracy and wide temporal coverage of CoRoT long runs, here LRA1, has allowed us for the first time to observe continuously a moderate outburst (several hundredths of magnitude) in the early Be star HD 49330. By analogy with the schematic picture of a line emission outburst described for μ Cen by Rivinius et al. (1998), we have proposed to divide the CoRoT light curve of HD 49330 into four parts: the relative quiescent, precursor, outburst, and relaxation phases.

For the first time, we have discovered a correlation between both amplitude changes and the presence/absence of certain frequencies of pulsations, with the different phases of an outburst. We have identified two kinds of changes: (i) the amplitude of the main frequencies (p modes) decreases before and during the outburst and increases again after the outburst; (ii) several groups of frequencies (g modes) appear just before the outburst, their amplitude reaches a maximum during the outburst, and they disappear as soon as the outburst has finished. These frequencies appear to have complex structures, which could represent pulsation modes with a short lifetime. We note that the frequency group around 0.87 c.d^{-1} is compatible with the rotation frequency $f_{\rm rot} = 0.94 \pm 0.20$ c.d^{-1} (Paper II). The emergence of this group of frequencies during the outburst may thus be explained by the ejection of material corotating with the star that did not reach a Keplerian orbit yet.

6.3. Correlation between pulsation and outburst

The correlation between the observed pulsations and the occurrence of the outburst is clear. Rivinius et al. (1998) proposed that the beating of non-radial pulsations are the origin of the Be phenomenon, i.e., the ejection of material into a circumstellar disk via outbursts. From spectroscopy, they found a correlation for μ Cen between the beating of pulsations and the strength of the emission lines. However, this result has not been reproduced for other Be stars up to now, maybe due to the lack of long continuous observing coverage. Our analysis of the CoRoT data of HD 49330 detects a correlation similar to that proposed by Rivinius et al. (1998) by means of a photometric analysis. It thus agrees with their hypothesis. However, one may also consider that it is the occurrence of the outburst that leads to the excitation of different modes, and not the converse. The exact timing of events would probably require a combined spectroscopic and photometric analysis over the full length of an outburst.

7. Conclusion

The long duration and high precision of the CoRoT photometric data has allowed, for the first time, the study of the pulsation modes of a Be star during the various phases of a light outburst. We found that variations in the amplitude of the pulsation p modes clearly correlated in time with the outburst, as well as g modes appearing mainly during the outburst phase. However, whether the variations in pulsation modes produce the outburst (as suggested by Rivinius et al. 1998) or whether the occurrence of the outburst leads to the excitation of modes, e.g., by means of a change in stellar structure, has still to be investigated. For this, a precise timing of the events with both spectroscopy and photometry obtained during the complete duration of an outburst would be necessary. Since CoRoT will observe other early Be stars in forthcoming runs, we may have the chance to observe more outbursts with CoRoT. Seismic modelling of HD 49330 will also be of great help.

Acknowledgements. The CoRoT space mission, launched on December 27th 2006, has been developped and is operated by CNES, with the contribution of Austria, Belgium, Brazil, ESA, Germany and Spain.

References

Appourchaux, T., Michel, E., Auvergne, M., et al. 2008, A&A, 488, 705
Baudin, F., Gabriel, A., & Gibert, D. 1994, A&A, 285, L29
Baudin, F., Gabriel, A., Gibert, D., Palle, P. L., & Regulo, C. 1996, A&A, 311, 1024
Floquet, M., Neiner, C., Janot-Pacheco, E., et al. 2002, A&A, 394, 137
Floquet, M., Hubert, A.-M., Huat, A.-L., et al. 2009, A&A, 506, 103
Frémat, Y., Zorec, J., Hubert, A.-M., & Floquet, M. 2005, A&A, 440, 305
Frémat, Y., Neiner, C., Hubert, A.-M., et al. 2006, A&A, 451, 1053
Gutiérrez-Soto, J., Fabregat, J., Suso, J., et al. 2007, A&A, 476, 927
Gutiérrez-Soto, J., Floquet, M., Samadi, R., et al. 2009, A&A, 506, 133
Hubert, A. M., & Floquet, M. 1998, A&A, 335, 565
Hubert, A. M., Floquet, M., & Zorec, J. 2000, in IAU Coll., 175, The Be Phenomenon in Early-Type Stars, ed. M. A. Smith, H. F. Henrichs, & J. Fabregat, ASP Conf. Ser., 214, 348
Kallinger, T., Reegen, P., & Weiss, W. W. 2008, A&A, 481, 571
Neiner, C., Floquet, M., Hubert, A. M., et al. 2005, A&A, 437, 257
Pojmanski, G. 2002, Acta Astron., 52, 397
Porter, J. M., & Rivinius, T. 2003, PASP, 115, 1153
Rivinius, T., Baade, D., Stefl, S., et al. 1998, A&A, 333, 125
Samadi, R., Fialho, F., Costa, J. E. S., et al. 2006, ESA SP 1306, 317, corrected in [arXiv:astro-ph/0703354]